Journal of Power Sources 185 (2008) 566–569

Contents lists available at ScienceDirect

Journal of Power Sources

journal homepage: www.elsevier.com/locate/jpowsour

Short communication

Nanostructured Mg_2Ni materials prepared by cold rolling and used as negative electrode for Ni–MH batteries

Sylvain Pedneault[a,b], Jacques Huot[b], Lionel Roué[a,*]

[a] INRS-Energie, Matériaux et Télécommunications, 1650 Boul. Lionel Boulet, C.P. 1200, Varennes, Québec, J3X 1S2 Canada
[b] Physics Department, Université du Québec à Trois-Rivières, 3351 Boul. des Forges, C.P. 500, Trois-Rivières, Québec, G9A 5H7 Canada

ARTICLE INFO

Article history:
Received 5 June 2008
Received in revised form 26 June 2008
Accepted 27 June 2008
Available online 6 July 2008

Keywords:
Metal hydrides
Magnesium
Nickel
Cold rolling
Ni–MH batteries

ABSTRACT

In the present work, cold rolling has been investigated as a new means of producing Mg-based metal hydrides for nickel–metal hydride (Ni–MH) batteries. Structure and electrochemical evolution of 2Mg–Ni cold-rolled samples were investigated as a function of the number of rolling passes as well as heat treatment. It was found that nanocrystalline Mg_2Ni alloy can be obtained by an appropriate three step process involving rolling, heat treatment and rolling again. It was shown that the number of primary and secondary rolling passes must be carefully optimized in order to favour the complete formation of Mg_2Ni alloy having a nanocrystalline structure (~10 nm in crystallite size) without excessive sample oxidation. Actually, the best result was obtained by first rolling 90 times, followed by a heat treatment at 400 °C for 4 h and roll again 20 times. The resulting material displayed an initial discharge capacity of 205 mAh g^{-1}, which is quite similar to that obtained with ball-milled Mg_2Ni alloy.

1. Introduction

Issues concerning climate change and air pollution are creating an increasing interest for low-emission vehicles such as hybrid electric vehicles (HEVs). The nickel–metal hydride (Ni–MH) battery is the dominant advanced battery technology for HEV applications due to its good overall performance, safety and environmental friendliness. However, initiatives must be taken to reduce the cost and to improve the performance of the Ni–MH battery system in order to favour consumer acceptance for the HEV. For that purpose, MH electrodes that are less expensive and that have higher energy–power densities than the usual $LaNi_5$-based materials used by the majority of the Ni–MH battery manufacturers have to be developed.

Recently, promising results have been obtained with Mg–Ni-based alloys prepared by mechanical alloying [1–3]. However, this synthesis process is rather expensive and not easily scalable. Therefore, it is important to put some effort on the elaboration of new and more efficient means of producing metal hydrides. From this perspective, cold rolling appears as an interesting alternative because this technique is simple, low cost, well known in the industry and easily scalable. Surprisingly, its application to metal hydride synthesis is relatively limited [4–11]. For instance, Zhang et al. [6] have demonstrated the beneficial effects of deformation by cold rolling on the hydrogen absorption/desorption behavior of the Ti–22Al–27Nb alloy. More recently, Ueda et al. [8] have shown the formation of Mg_2Ni alloy by a combination of cold rolling and heat treatment. It was observed that the maximum H/M value was higher and the activation time for hydrogenation was shortened for laminated Mg_2Ni material than that of as-cast Mg_2Ni specimen. Furthermore, cold rolling has shown the possibility of enhancement for hydrogen sorption kinetics and air resistance for Mg–Pd-based hydrides compared to that of ball-milled samples [9,10].

In the present study, nanocrystalline Mg_2Ni alloy was obtained by a three step process involving cold rolling, heat treatment and further cold rolling. The structural evolution of the Mg:Ni (2:1) material was studied by X-ray diffraction (XRD) as a function of number of rolling passes and subsequent heat treatments. The hydrogen discharge capacities of the resulting Mg_2Ni alloys were determined. To the best of our knowledge, this is the first application of cold rolling for preparing Mg-based hydrogen storage materials for Ni–MH batteries

2. Experimental

Magnesium foil was prepared by cutting a small piece from a commercial ingot (Norsk Hydro) and rolling it to 0.3 mm thickness. The nickel foil was from Aldrich (0.125 mm thick, 99.9+%). Alternate Mg and Ni foils were stacked to get the appropriate stoichiometry. The stack was inserted between two stainless steel (316) plates and

* Corresponding author. Tel.: +1 450 929 8185; fax: +1 450 929 8102.
E-mail address: roue@emt.inrs.ca (L. Roué).

0378-7753/$ – see front matter © 2008 Elsevier B.V. All rights reserved.
doi:10.1016/j.jpowsour.2008.06.077

rolled in air in a conventional rolling mill with 55-mm diameter rolls. After each roll, the foil was folded in two and rolled again thus giving a 50% thickness reduction at each rolling pass. Final thickness of the foil was 0.45 mm. All handling were performed in air. Heat treatment was performed at 400 °C in a tubular furnace under argon flow for a period of 4 h. For comparison, nanocrystalline Mg_2Ni alloy was synthesized by ball milling from elemental Mg and Ni powders. The ball milling was performed under argon for 10 h using a vibratory type mill (SPEX 8000 Mixer) with a ball-to-powder mass ratio of 10:1.

X-ray diffraction patterns were obtained on a Rigaku D-max diffractometer using Cu Kα radiation. The XRD profiles were treated by Rietveld refinement using EXPGUI and GSAS softwares [12,13]. The oxygen and nitrogen contents in the samples were measured with a TC-136 oxygen/nitrogen detector from LECO.

The electrochemical tests were performed at room temperature on a Voltalab 40 (Radiometer Analytical) potentiostat/galvanostat/FRA apparatus, using a three electrode cell filled with a 6 M KOH electrolyte solution. Working electrodes were made by pressing the as-rolled material between two nickel foams. In the case of the ball-milled 2Mg + Ni sample, the working electrode was made from a mixture of 100 mg of Mg_2Ni powder plus 800 mg of graphite and 20 mg of carbon black. Nickel wire and Hg/HgO electrode (XR440 from Radiometer Analytical) were used as counter and reference electrode, respectively. The working electrode was charged at 200 mA g^{-1} for 3 h and discharged at 20 mA g^{-1} up to −0.6 V vs. Hg/HgO. All samples were stored in air prior to electrochemical tests.

3. Results and discussion

3.1. Crystal structure

In the present investigation, nanocrystalline Mg_2Ni alloy was obtained by a three step process involving rolling, heat treatment and rolling again. After 90 primary rolling passes (Fig. 1A) of a 2Mg + Ni stack, only magnesium and nickel phases were present. It is observed that magnesium is highly oriented toward (0 0 2) direction, while nickel is oriented along (2 2 0) and (3 1 1). Crystal sizes are very similar for both elements being around 115 nm. Microstrain is present in both phases: 0.78% for magnesium and 0.42% for nickel.

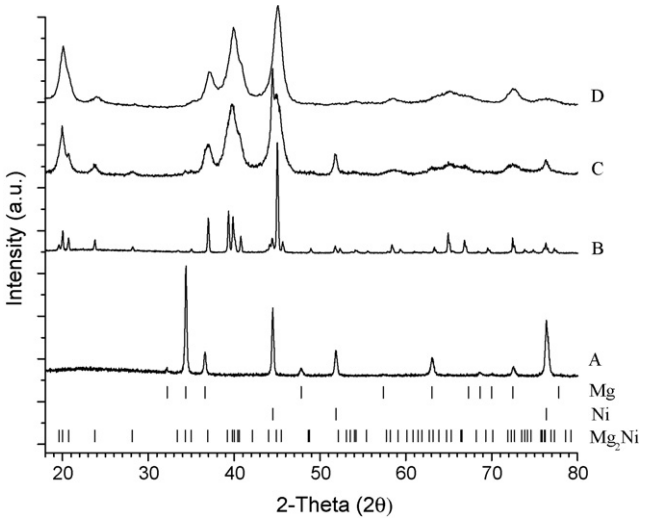

Fig. 1. X-ray patterns of 2Mg + Ni after 90 primary rolling passes (A); 90 primary rolling passes and heat treatment (B); 90 primary rolling passes, heat treatment and 20 secondary rolling passes (C). For comparison, X-ray pattern of the 10 h ball-milled 2Mg + Ni mixture is shown (D).

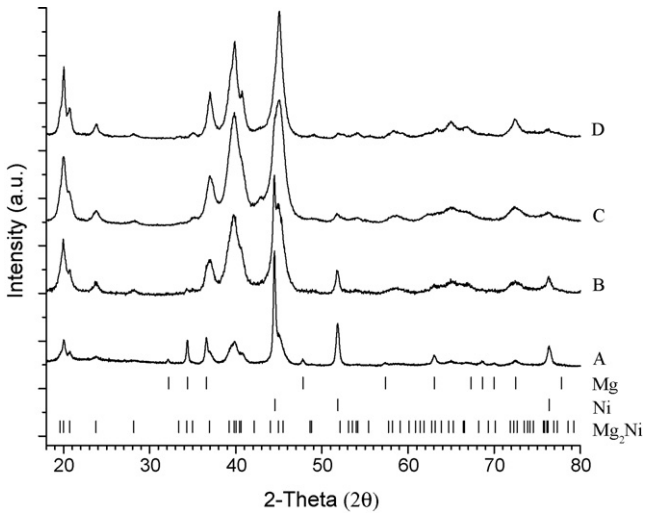

Fig. 2. X-ray patterns of 2Mg + Ni when 60 (A), 90 (B), 150 (C) and 180 (D) primary rolling passes are done, followed by heat treatment and 20 secondary rolling passes.

As shown in Fig. 1B, after heat treatment the material is mainly composed of Mg_2Ni, the rest being unalloyed Ni. From Rietveld analysis, the material is made of 87 wt.% Mg_2Ni having an average crystallite size of 209 nm and 13 wt.% of nickel with a crystallite size of 70 nm. No microstrain is observed in the heat-treated material.

Once the Mg_2Ni phase is formed, 20 secondary rolling passes had a drastic effect on crystallite size as seen by the very broad peaks of Fig. 1C. From Rietveld analysis it was found that crystallite size of Mg_2Ni decreased to 9 nm while for nickel, the crystallite size was reduced to 28 nm. This indicates that secondary rolling is a very effective means of reducing crystallite size. For comparison, Fig. 1D shows the XRD pattern of the 10 h ball-milled 2Mg + Ni mixture. We see that the diffraction pattern is identical with respect of the Mg_2Ni phase observed in Fig. 1C. The only difference is the absence of free nickel in the milled sample.

The effect of primary (before heat treatment) and secondary (after heat treatment) rolling processes on the end product structure was investigated. The effect of the number of primary rolling passes on the final structure is shown in Fig. 2. In this experiment, after a number of primary rolling passes varying from 60 to180, all

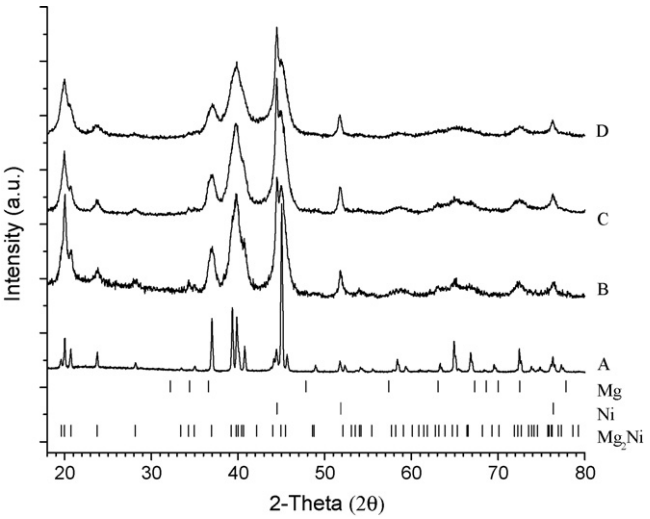

Fig. 3. X-ray patterns of 2Mg + Ni when 90 primary rolling passes are followed by heat treatment and 0 (A), 10 (B), 20 (C) and 50 (D) secondary rolling passes.

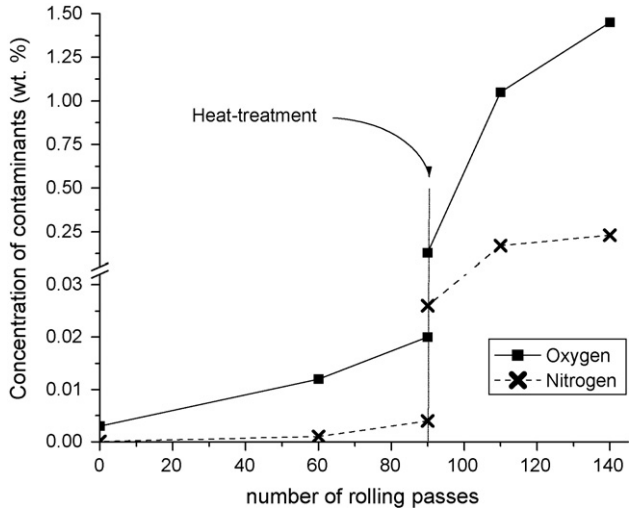

Fig. 4. Variation of the concentration of oxygen and nitrogen contaminants as a function of the number of rolling passes.

samples were heat treated and subjected to the same number of secondary rolling passes (20). It could be seen that at least 90 primary rolling passes are needed before all the magnesium is alloyed to nickel to form the Mg_2Ni phase. Increasing the number of primary rolling passes has almost no effect on the structure of the Mg_2Ni phase.

The effect of secondary rolling treatment on the product structure is shown in Fig. 3. In this experiment, the samples were first rolled 90 times (primary rolling), heat treated and then subjected to various numbers of secondary rolling passes (0, 10, 20 and 50). After only 10 secondary rolls, the crystallite size of Mg_2Ni is already reduced to 12 nm. However, further rolling only marginally decreases the crystallite size and increases microstrain. After 50 secondary rolls, the Mg_2Ni phase shows an average crystallite size of 8 nm and a microstrain of 2.2%.

As all our manipulations are done in air, sample oxidation could be important. Fig. 4 displays the evolution of oxygen and nitrogen contents during primary rolling, heat treatment and secondary rolling. Primary rolling does not have a large impact on the sample contamination. Oxygen level goes from 0.004 wt.% for the starting materials to 0.02 wt.% after 90 rolls. Nitrogen contamination is even lower. However, a 10-fold increase (please note the change of scale on the graph) of oxygen and nitrogen contamination occurs during heat treatment despite the fact that argon gas was always flowing inside the furnace. After heat treatment the samples are much more sensitive to air as indicated by the important increases of contamination as a function of the number of secondary rolling passes. The reason for such behavior may be due to a higher sensitivity of the Mg_2Ni phase to oxygen than the unalloyed Mg and Ni phases.

3.2. Electrochemical performance

Fig. 5 shows a typical charge–discharge curve (first cycle) of cold-rolled Mg_2Ni electrode. During charge (at 200 mA g^{-1} during 3 h), the potential decreases progressively from −0.92 to −1.04 V vs. Hg/HgO, reflecting the occurrence of the hydrogen absorption reaction. After 2 h of charge, the Mg_2Ni electrode is fully charged and then the potential stabilizes around −1.04 V vs. Hg/HgO, due to the hydrogen evolution reaction. During the discharge step (at 20 mA g^{-1} up to −0.6 V vs. Hg/HgO), the electrode potential

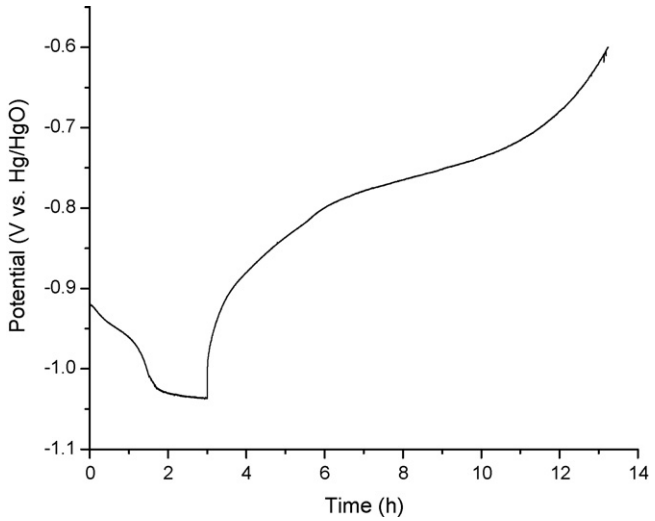

Fig. 5. Typical charge–discharge curve (first cycle) of cold-rolled Mg_2Ni electrode (90 primary rolling passes, heat treatment at 400 °C and 20 secondary rolling passes). Charge at 200 mAh g^{-1} for 3 h and discharge at 20 mAh g^{-1} up to −0.6 V vs. Hg/HgO.

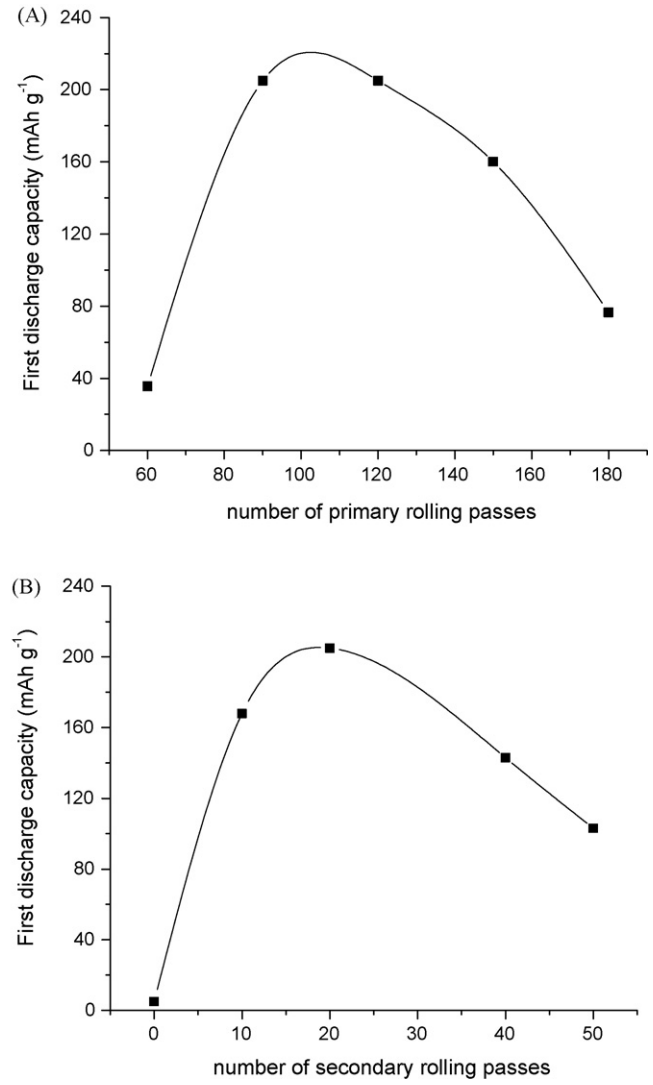

Fig. 6. (A) Variation of the first discharge capacity as a function of the number of primary rolling passes. In this case, 20 rolling passes were done after heat treatment. (B) Variation of the first discharge capacity as a function of the number of secondary rolling passes. In this case, 90 rolling passes were done prior to heat treatment.

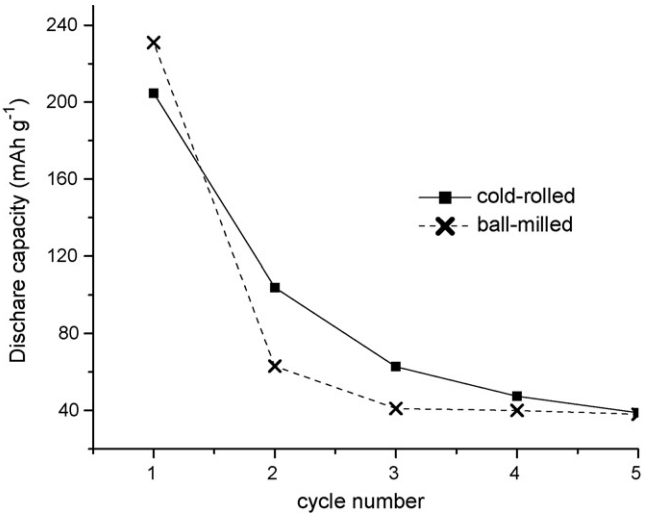

Fig. 7. Cycling discharge capacities of 2Mg + Ni samples ball milled 10 h and cold rolled (90 primary rolling passes, heat treatment at 400 °C and 20 secondary rolling passes).

increases slowly with a quasi-plateau around −0.8 V vs. Hg/HgO related to the β-to-α phase transition. When the hydrogen desorption reaction is completed, a rapid increase of the potential is observed. On the basis of the discharge duration, the discharge capacity of the material can be estimated (205 mAh g^{-1} in the present case).

The electrode discharge capacity (first cycle) depends on both primary and secondary rolling pass numbers as seen in Fig. 6A and B, respectively. On the basis of our previous characterizations, too many rolling passes result in more sample oxidation. On the other hand, a too low number of primary rolling passes yields to a partial formation of Mg_2Ni intermetallic compound. Moreover, an insufficient number of secondary rolling passes results in a too large Mg_2Ni crystallite size. The highest discharge capacity (205 mAh g^{-1}) is then obtained by first rolling 90 or 120 times, followed by a heat treatment and then roll again 20 times.

Fig. 7 shows the variation of the discharge capacity upon cycling for our best cold-rolled sample and the ball milled one. As can be seen, the results are quite the same for both electrodes in terms of initial discharge capacity and decay capacity with cycling. Indeed, the initial discharge capacity of the cold-rolled Mg_2Ni electrode is 205 mAh g^{-1} with a decay capacity of 81% after 5 cycles compared to an initial discharge capacity of 231 mAh g^{-1} and a decay capacity of 83% after 5 cycles for the ball-milled Mg_2Ni sample. In comparison, Mg_2Ni electrode fabricated from 25 h ball-milled Mg_2Ni alloy (intermetallic phase already formed before ball milling) displayed an initial discharge capacity of 244 mAh g^{-1} with a decay capacity of 72% after 25 cycles whereas unmilled (polycrystalline) Mg_2Ni alloy was inactive with a maximum discharge capacity of 2 mAh g^{-1} [14].

The data in Fig. 7 suggests that the cold-rolled material exhibits a slower loss of discharge capacity on cycling than the ball-milled material. However, for both cold-rolled and ball-milled materials, the discharge capacity is reduced to ∼40 mAh g^{-1} after 5 cycles that prohibit their use in Ni–MH batteries. The rapid decay capacity with cycling is well known for Mg-based materials and is attributed to $Mg(OH)_2$ formation [2]. Actually, Mg_2Ni undergoes spontaneous hydrolysis in water and in hydroxide solutions ($\Delta G^\circ = -544$ kJ mol^{-1}) [15]. The accumulation of $Mg(OH)_2$ on the electrode limits the hydrogen absorption/desorption reaction in addition to consuming active material. Thus, more works needs to be done in order to get better cycle life, as successfully done with ball-milled MgNi-based materials [3].

4. Conclusion

This work showed that cold rolling combined with heat treatment could be a promising synthesis method of nanostructured metal hydrides. It has enabled us to get a nanocrystalline Mg_2Ni material in sheet form which displays similar electrochemical hydrogen storage properties to that of nanocrystalline Mg_2Ni powder obtained by ball milling.

Acknowledgements

This work was supported by the Fonds Québécois de la Recherche sur la Nature et les Technologies (FQRNT) and the Natural Sciences and Engineering Research Council (NSERC) of Canada.

References

[1] S. Ruggeri, C. Lenain, L. Roué, G. Liang, J. Huot, R. Schulz, J. Alloys Compd. 339 (2002) 195.
[2] S. Ruggeri, L. Roué, R. Schulz, L. Aymard, J.M. Tarascon, J. Power Sources 112 (2002) 547.
[3] C. Rongeat, S. Ruggeri, M.-H. Grosjean, M. Dehmas, S. Bourlot, L. Roué, J. Power Sources 158 (2006) 747.
[4] T. Ben Ameur, A.R. Yavari, Collq. Phys. C4 (1990) 219.
[5] T. Ben Ameur, A.R. Yavari, J.M. Barandiaran, Mater. Sci. Eng. A 134 (1991) 1402.
[6] L.T. Zhang, K. Ito, V.K. Vasudevan, M. Yamaguchi, Acta Mater. 49 (2001) 751.
[7] L.T. Zhang, K. Ito, V.K. Vasudevan, M. Yamaguchi, Mater. Sci. Eng. A 329–331 (2002) 362.
[8] T.T. Ueda, M. Tsukahara, Y. Kamiya, S. Kikuchi, J. Alloys Compd. 386 (2005) 253.
[9] J. Dufour, J. Huot, J. Alloys Compd. 439 (2006) L5.
[10] J. Dufour, J. Huot, J. Alloys Compd. 446–447 (2007) 147.
[11] N. Takeichi, K. Tanaka, H. Tanaka, T.T. Ueda, Y. Kamiya, M. Tsukahara, H. Miyamura, S. Kikuchi, J Alloys Compd. 446–447 (2007) 543.
[12] A.C. Larson, R.B. Von Dreele, in: General Structure Analysis System (GSAS), Report LAUR 86-748, Los Alamos National Laboratory, 2000.
[13] B.H. Toby, J. Appl. Crystallogr. 34 (2001) 210.
[14] H. Niu, D.O. Northwood, Int. J. Hydrogen Energy 27 (2002) 69.
[15] H. Wang, D.O. Northwood, Int. J. Mater. Sci. 43 (2008) 1050.